

Imprinting Light Phase on Matter Wave Gratings in Superradiance Scattering

Xiaoji Zhou,^{1,*} Fan Yang,¹ Xuguang Yue,¹ T. Vogt,¹ and Xuzong Chen^{1,†}

¹*School of Electronics Engineering & Computer Science,
Peking University, Beijing 100871, P. R. China*

(Dated: November 23, 2018)

Superradiance scattering from a Bose-Einstein condensate is studied with a two-frequency pumping beam. We demonstrate the possibility of fully tuning the backward mode population as a function of the locked initial relative phase between the two frequency components of the pumping beam. This result comes from an imprinting of this initial relative phase on two matter wave gratings, formed by the forward mode or backward mode condensate plus the condensate at rest, so that cooperative scattering is affected. A numerical simulation using a semiclassical model agrees with our observations.

PACS numbers: 03.75.Kk, 42.50.Gy, 42.50.Ct, 32.80.Qk

Superradiance from a Bose-Einstein Condensation (BEC) offers the possibility of studying a novel physics associated with cooperative scattering of light in ultracold atomic systems. A series of experiments [1–4] and related theories [5–7] have sparked new interests in matter wave amplification [1, 2], holographic storage [4], scattering spectroscopy in optical lattice [8], coherent imaging [9], coherent atomic recoil lasing [10–12], and quantum states storage and retrieval [13, 14].

In a typical BEC superradiance experiment, an elongated condensate is illuminated by an off-resonant pumping laser pulse along its short axis. Due to the phase-matching condition and mode competition, highly directional light is emitted along the long axis of the condensate, in the so-called end-fire modes. Consequently, the recoiled atoms acquire a well-defined momentum at $\pm 45^\circ$ angles with respect to the pumping laser direction. These atomic modes are referred to as forward modes. This forward scattering is interpreted as optical diffraction from a matter wave grating [1, 5]. Meanwhile, atoms in the condensate may scatter photons in the end-fire modes back into the pumping mode and recoil at $\pm 135^\circ$ angles, forming the so-called backward modes [3, 7], when the pumping pulse is short and intense. This pattern was interpreted as a result of diffraction of atoms off a light grating. A four wave mixing interpretation was proposed, involving two optical fields—the pumping laser field and an end-fire mode, and two matter wave modes—the condensate and a mode of momentum [7].

There is an energy mismatch of four times the recoil frequency for this backward scattering, due to the increased kinetic energy of recoiled atoms [3, 6]. Recently, a two-frequency-pumping scheme has been implemented [15–17], where the pumping beam consisted of two frequency components and the frequency difference was controlled to compensate for the energy mismatch

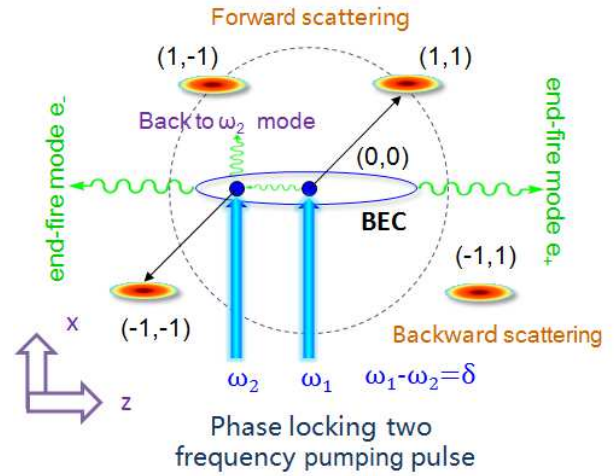


FIG. 1. (Color online) Schematic diagram of our experiment. The two-frequency pumping beam is incident along the short x direction, with a linear polarization along the y direction. The atomic side modes are denoted in momentum space, each labeled with a pair of integers which describe the order in the x and z directions, respectively. Within this notation, atoms of the condensate at rest are in mode $(0,0)$. A forward scattering event transfers an atom from mode (n,m) to mode $(n+1,m\pm 1)$, and a backward event transfers one to mode $(n-1,m\pm 1)$. The end fire mode e_{\pm} is along the long axis of the condensate in z direction.

and excite the backward scattering on a long time scale with a weak pump intensity. The presence of the backward mode in the spectroscopic response [16] and the enhancement of the diagonal sequential scattering [17] have been reported. In those experiments the relative phase between the two pumping frequency components is maintained constant. Although phase is a very important factor for understanding interference and coherence phenomena, phase effects on matter wave gratings and cooperative scattering have not been reported so far.

We present here our new experimental results that

* E-mail: xjzhou@pku.edu.cn

† E-mail: xuzongchen@pku.edu.cn

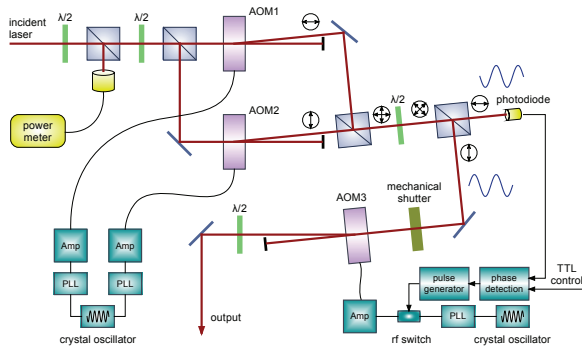


FIG. 2. Two-frequency superradiance scattering experimental setup. The pump laser beam is split into two beams with orthogonal polarizations using a PBS. With two AOMs, each beam frequency is shifted about 90 MHz, with a little difference of $\Delta\omega$. In order to keep the coherence of the two beams after frequency shifting, the phase-locked-loops of the radio frequency (rf) sources for the two AOMs are locked to the same crystal oscillator. A phase detection circuit is used to detect the initial relative phase of beating signal of the two frequency beams after they are combined. Note that the beat signal of the pump pulse is opposite in phase with the signal measured by the photodiode.

show a possibility to fully control the backward mode population as a function of the locked initial relative phase between the two pumping frequencies. A theoretical analysis of the cooperative process is used to confirm and explain this phase dependence. It requires to consider the relationship between matter wave gratings and optical waves beating for the first order scattering. The initial relative phase of the pumping beam is imprinted into two matter wave gratings, one formed by the condensate with a forward mode, the other formed by the condensate with a backward mode.

In our experiment, a nearly pure Bose-Einstein condensate of about 2×10^5 ^{87}Rb atoms in the $|F = 2, m_F = 2\rangle$ hyperfine ground state is generated in a quadrupole-Ioffe-configuration magnetic trap, with Thomas-Fermi radii of $50\mu\text{m}$ and $5\mu\text{m}$ along the axial and radial directions [17]. The pumping pulse with two-frequency components is incident along the short axis of the condensate, with its polarization perpendicular to the long axis, as shown in Fig. 1. This arrangement of polarization induces Rayleigh superradiance where all side modes possess the same atomic internal state [1]. To get the two-frequency pumping beam, a laser beam from an external cavity diode laser is split into two equal-intensity beams. Their frequencies are shifted individually by acousto-optical modulators (AOM1 and AOM2) which are driven by phase-locked radio frequency signals. Therefore the frequency difference $\Delta\omega$ between the two beams can be controlled precisely, as shown in Fig. 2. After that, they are recombined to form our linear-polarized two-frequency pump beam, which is red detuned by $2\pi \times 1.5\text{GHz}$ from

the $|F = 2, m_F = 2\rangle$ to $|F' = 3, m'_F = 3\rangle$ transition.

The frequency difference $\Delta\omega$ is chosen to be $2\pi \times 15\text{kHz}$ (the corresponding period T is then $66.67\mu\text{s}$), i.e. four times the recoil frequency ($4\omega_r = 2\hbar k_i^2/M$) so that we reach the two-photon resonance condition taking into account the recoil energies deficit for the backward scattering. The magnetic trap is shut off immediately after the pumping pulse, and the distribution of atomic side modes is measured by absorption imaging after 21ms of ballistic expansion, as shown in Fig. 3.

The experiment is repeated with different initial relative phases between the two frequency components. Monitoring the beating signal $\cos(\Delta\omega t + \phi)$ on a photodiode, a light pulse of duration T with a definite initial relative phase $\phi_0 = \Delta\omega t_0 + \phi$ can be generated. Different initial relative phases ϕ_0 varying between 0 and 2π , are obtained by switching on the pulse at different time t_0 , which we call “generation time”, as shown in Fig. 3(e). The generation time t_0 and the switch off time $t_0 + T$ can be controlled precisely with an AOM. Figure 3(a) and (b) demonstrate the initial relative phases of the two frequency pumping beam being $\pi/2$ and 1.4π , the corresponding generation time t_0 being $50\mu\text{s}$ and $20\mu\text{s}$, respectively. This phase can be read out related to the reference signal corresponding to $\phi_0 = 0$.

In Fig. 3 (c), the backward mode is obvious for a relative initial phase $\phi_0 = \pi/2$ while in Fig. 3 (d), when the phase is $\phi_0 = 1.4\pi$, backward scattering is almost suppressed. The ratio between the backward population and the total atom number is plotted in Fig. 4 versus different phases ϕ_0 , with a pulse duration equal to $66.67\mu\text{s}$ or one cycle, a time step between two points given by $\Delta t_0 = 10\mu\text{s}$ and each point being the average on four experimental data. The error bar is their standard deviation. For each experiment, the atom number in the BEC, the initial quantum noise and the temperature are not exactly the same. These fluctuations are the main reason for the experimental uncertainty. Nevertheless, the number of backward scattered atoms shows a high sensitivity to the initial relative phase between the two frequency components and it is possible to obtain an almost complete cancellation of the backward scattering for $\phi_0 = 3\pi/2$.

Such a result was not expected considering in particular the interpretations given in previous experiments. Especially, the exponential growth model of scattered atoms used in previous articles [1] would not accurately account for the phase dependence. Even considering the depletion of the original mode of the condensate it writes $dN_s(t)/dt = G(t)(N_0 - N_s(t))N_s(t)$, where N_s is the number of scattered atoms and N_0 the initial number of atoms in the condensate [1]. The gain $G(t)$ is proportional to the pump intensity $I(t)$. This logistic differential equation can be solved analytically as $N_s(t) = [N_0 e^{N_0 \int_0^t G(t) dt}] / [N_0 - 1 + e^{N_0 \int_0^t G(t) dt}]$. Within this model, the number of scattered atoms is determined by the integration of the pump intensity $I(t)$, thus pro-

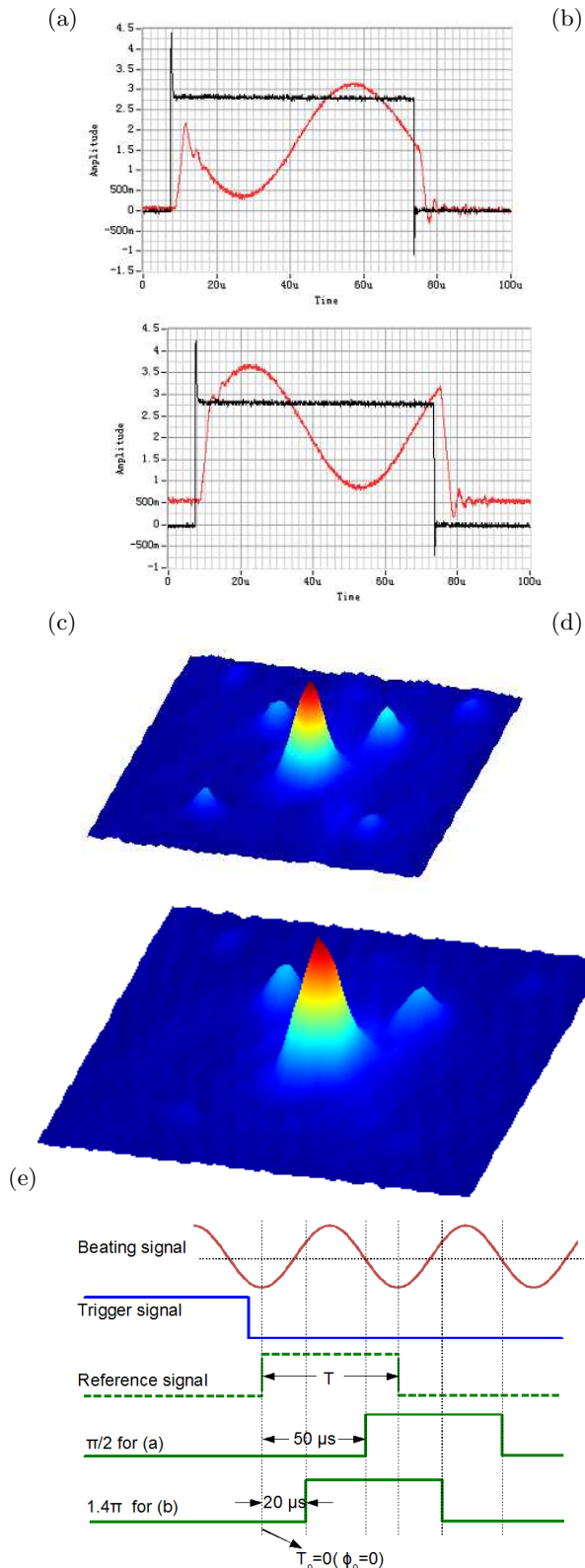


FIG. 3. Superradiance with different initial relative phases and time control sequence. (a) and (b): Initial relative phase of $\pi/2$ and 1.4π corresponding to a generation time of $50\mu\text{s}$ and $20\mu\text{s}$ respectively. (c) and (d): Superradiance patterns corresponding to (a) and (b), respectively. (e) Control sequence for generating the pump pulse. Note that there is a phase difference of π between the phase shown in figures (a) and (b) and that of the real pumping pulse.

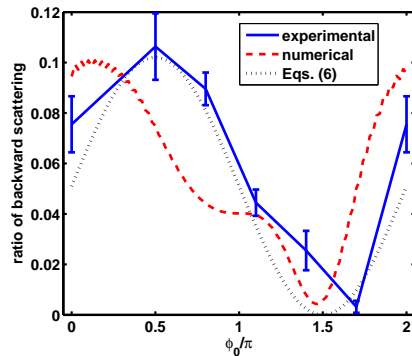


FIG. 4. (Color online) Experimental results and theoretical analysis about the ratio of backward scattered atoms to the total atom number vs the initial phase ϕ_0 between the two pump beams. Each point is an average on four experimental data. The dashed line is a numerical simulation using a semiclassical theory depicted in the text with one initial seed and c coupling factor $g = 1.5 \times 10^6$. The dotted line is drawn using Eq.(6) with $\Delta\varphi_{0,1} = \pi/2$.

portional to $\int_0^t I(t)dt = I_0 \int_0^t [1 + \cos(\Delta\omega t + \phi_0)]dt \geq 0$. When the pumping pulse duration equals to an exact cycle, the integration of the pump intensity is always the same, regardless of the relative initial phase between the two frequency components. This means, within this nonlinear growth model, the number of scattered atoms is independent of the initial relative phase.

The above model is not valid since more than one scattered mode should be taken into account. Actually, the different modes form matter wave gratings and affect the scattering behavior. To give a physical explanation, we need to clarify the relationship between the population of the different modes and the initial relative phase ϕ_0 . Here we restrain our analysis to a set of diagonal modes: $(-1, -1)$, $(0, 0)$, and $(1, 1)$. Results are similar for the other diagonal modes $((1, -1)$, $(0, 0)$, and $(-1, 1))$ because of symmetry. Using the slowly varying envelope approximation (SVEA) [6], the population of mode $(-1, -1)$ is given by its wave function $\psi_{-1,-1}(\xi, \tau)$:

$$\frac{\partial N_{-1,-1}(\tau)}{\partial t} = \int_{-\infty}^{\infty} d\xi \left(\frac{\partial \psi_{-1,-1}}{\partial t} \psi_{-1,-1}^* + \frac{\partial \psi_{-1,-1}^*}{\partial t} \psi_{-1,-1} \right). \quad (1)$$

We use the semiclassical Maxwell-Schrödinger equations to describe the coupled dynamics of matter-wave and optical fields. Although this theory can not be used to analyze the initial quantum spontaneous process, the pulse in the experiment is about several tens of μs and far beyond its initial quantum characteristic. So the effect of the pump beam phase on the initial seeds can be omitted to analyze the experimental data [6, 16, 17]. Considering the trapped BEC is tightly constrained at its short axis degrees and the Fresnel index number of the optical field is around 1, we consider a one-dimensional semiclassical model including spatial propagation effects. Then

the envelope function of the end-fire mode optical fields with a pump laser consisting of two components having same intensity and polarization but different frequencies $\omega_l = ck_l$ and $\omega_l - \Delta\omega$, is given by [6, 17]

$$e_-(\xi, \tau) = -i\kappa(\phi_0)\sqrt{\frac{L}{k_l}}\int_{\xi}^{\infty} d\xi'(\psi_{0,0}\psi_{1,1}^* + \psi_{-1,-1}\psi_{0,0}^*e^{-i2\tau}), \quad (2)$$

where $\tau = 2\omega_r t$ and $\xi = k_l z$. $\kappa(\phi_0) = g(1 + e^{i(2\tau + \phi_0)})$ is connected with the initial relative phase ϕ_0 and the coupling factor between light and atom $g = \sqrt{3\pi cR/(2\omega_l^2 AL)}$. R is the Rayleigh scattering rate of the pump component and L the BEC length. It indicates that the end-fire mode field e_- is due to the coherence between different modes, such as modes (0,0) and (1,1), (-1,-1) and (0,0), and spatial overlap between these modes is needed. There exists $4\omega_r$ frequency difference between adjacent modes.

The coupled evolution equations of atomic side modes is given by

$$\frac{\partial\psi_{-1,-1}(\xi, \tau)}{\partial\tau} = -i\kappa^*(\phi_0)e_-\psi_{0,0}e^{i2\tau} \quad (3)$$

This equation describes the atom exchange between modes (-1,-1) and (0,0) through the pump laser and end-fire mode field. An atom in (-1,-1) mode may absorb a laser photon and emit it into an end-fire mode e_- , and the accompanying recoil drives the atom into the (0,0) mode. The atom may absorb an endfire mode photon and deposit it into the laser mode, to form the backward scattering mode (-2,-2) which process is very weak and omitted. Here we have omitted the dispersion term, spatial translation, photon exchange between modes and non-diagonal modes connected with e_+ such as mode (-2,0) and (0,-2) [6, 17].

Inserting Eq. (2) and (3) into Eq. (1), we can get the evolution equation of $N_{-1,-1}$

$$\frac{\partial N_{-1,-1}(\tau)}{\partial\tau} = -2\frac{g^2 Lc}{\omega_r c}[1 + \cos(2\tau + \phi_0)] \times [C_{0,1}e^{i2\tau} + C_{-1,0}] + c.c., \quad (4)$$

where the envelope function of each side mode $\psi_{m,m}$ is written as $\psi_{m,m} = |\psi_{m,m}|e^{-i\varphi_{m,m}}$ with the phase $\varphi_{m,m}$ assumed to be space independent. Here we define $C_{m,n}(\tau) = \int_{-\infty}^{\infty} d\xi \tilde{C}_{m,n}(\xi, \tau) = |C_{m,n}(\tau)|e^{-i\Delta\varphi_{m,n}}$ with the phase difference between the matter waves $\Delta\varphi_{m,n} = \varphi_{m,m} - \varphi_{n,n} + \varphi_{0,0} - \varphi_{-1,-1}$, and the interference grating $\tilde{C}_{m,n}(\xi, \tau) = \psi_{0,0}\psi_{-1,-1}^* \int_{\xi}^{\infty} d\xi' \psi_{m,m}\psi_{n,n}^*$. Then we have $\Delta\varphi_{0,1} = 2\varphi_{0,0} - \varphi_{1,1} - \varphi_{-1,-1}$, and $\Delta\varphi_{-1,0} = 0$.

In this case the above Eq. (4) can be expanded using trigonometric formula

$$\frac{\partial N_{-1,-1}(\tau)}{\partial\tau} = -\frac{g^2 L}{\omega_r c} \{ [|C_{0,1}|2\cos(2\tau - \Delta\varphi_{0,1}) + \cos(\phi_0 + \Delta\varphi_{0,1}) + \cos(4\tau + \phi_0 - \Delta\varphi_{0,1})] + 2|C_{-1,0}|[1 + \cos(2\tau + \phi_0)] \} \quad (5)$$

In a first approximation, we replace $|C_{m,n}|$ by its time average $\overline{|C_{m,n}|}$. Equation (5) can then be integrated from 0 to one cycle, and the cosine functions of time vanish, leaving only the $\cos(\phi_0 + \Delta\varphi_{0,1})$ term. A simpler expression for $N_{-1,-1}$ at the end of the pumping pulse ($\Delta\omega t = 2\pi$ or $\tau = \pi$) is obtained:

$$N_{-1,-1}(\pi) = -2\pi\frac{g^2 L}{\omega_r c}\overline{|C_{0,1}|}\cos(\phi_0 + \Delta\varphi_{0,1}) + \alpha, \quad (6)$$

The first term of Eq. (6) indicates that the population of side mode (-1,-1) is connected with the module of four waves $|C_{0,1}| = |\psi_{0,0}\psi_{-1,-1}^*| \int_{\xi}^{\infty} d\xi' |\psi_{0,0}\psi_{1,1}^*|$, the relative phase $\Delta\varphi_{0,1}$ and the optical initial relative phase ϕ_0 , the coefficient of the cosine function determining the amplitude of the oscillation. The second part α approximated to be a constant in the above expression should actually include other terms due to the residual time dependent part of $|C_{m,n}|$ and may also slightly depend on ϕ_0 . This dependence may be neglected in a first approximation as the time-dependent terms in Eq. (5) have different time-dependent signatures and may cancel each other after integration. The main purpose of Eq. (6) is to show the dependence of the backward scattering on the initial relative phase ϕ_0 , although it is hard for us to prove its positivity due to the complexity of α . However, numerical calculations demonstrate that this backward scattered atom number is always positive.

To give a physical explanation to this initial relative phase dependence and because of the assumption that the phase $\varphi_{m,m}$ of each side mode does not depend on space, we can focus our attention on the terms $\tilde{C}_{m,n}$ since the spatial integral from $-\infty$ to ∞ in the definition of $C_{m,n}$ does not change the relative phase of the matter waves. The term $\tilde{C}_{0,1} = \psi_{0,0}\psi_{-1,-1}^* \int_{\xi}^{\infty} d\xi' \psi_{0,0}\psi_{1,1}^*$ indicates the presence of two sequential diffractions by two gratings, which we analyze as follows. With the spatial coordinates described in Fig. 1, the incident laser light traveling in the x direction is diffracted by the grating formed by modes (0,0) and (1,1), which is along the diagonal of the $x-z$ plane, and can be expressed as $\int_z^{\infty} dz |\psi_{0,0}\psi_{1,1}^*| \cos(kx + kz + \varphi_{1,1} - \varphi_{0,0})$. The scattered light (end-fire mode light) propagating along the long axis of the condensate in $-z$ direction is then diffracted again by the grating formed by modes (0,0) and (-1,-1), which is also along the diagonal of the $x-z$ plane, and can be described as $|\psi_{0,0}\psi_{-1,-1}^*| \cos(kx + kz - \varphi_{-1,-1} + \varphi_{0,0})$, resulting in a scattered light traveling back into x direction which is highly correlated to the backward scattered atom number. The spatial integral in the former grating describes the propagating effect. Here a phase shift of $\pi/2$ takes place as the integral can be approximated to be $-|\psi_{0,0}\psi_{1,1}^*| \sin(kx + kz + \varphi_{1,1} - \varphi_{0,0}) = |\psi_{0,0}\psi_{1,1}^*| \cos(kx + kz + \varphi_{1,1} - \varphi_{0,0} + \pi/2)$. Based on light diffraction theory, when a beam is incident at an angle of 45° onto a grating, which is the combination of two gratings, the maximum diffraction light along the incident direction occurs when these two gratings are in phase.

That is, $-\varphi_{-1,-1} + \varphi_{0,0} = \varphi_{1,1} - \varphi_{0,0} + \pi/2$, or

$$(\varphi_{1,1} - \varphi_{0,0}) + \frac{\pi}{2} + (\varphi_{-1,-1} - \varphi_{0,0}) = 0. \quad (7)$$

That means $\Delta\varphi_{0,1} = \pi/2$. According to our simulation we find that the relative phase of the matter waves $\Delta\varphi_{0,1}$ is nearly $\pi/2$, and there is a little deviation for different initial relative phases ϕ_0 of pump beam. The dependence of $\Delta\varphi_{0,1}$ on ϕ_0 reflects the intrinsic nature of nonlinearity in the superradiance process since it should not depend on the initial relative phase between the two frequency components when the pumping pulse duration equals to an exact cycle for a linear process. The initial relative phase of the pumping beams slightly alters the phase matching condition, which maybe results in the divergence between our simple model and the numerical result. However, in our discussed model, the result giving $\Delta\varphi_{0,1} = \pi/2$ is reasonable and meaningful for understanding the scattering picture.

According to Eq. (6) and (7) and neglecting α , the ratio of backward scattered atoms to the total atom number versus the initial phase ϕ_0 is simply a sinusoidal function and is plotted as the dotted line in Fig. 4, with its amplitude adjusted to the experimental data. Backward scattering is enhanced when the relative phase is nearly $\phi_0 = \pi/2$, while suppressed for ϕ_0 close to $3\pi/2$. This simple model agrees well with our experimental data except for a small shift of the minimum.

Furthermore, the ratio of the backward scattering atom number to the total atom number is simulated numerically using coupled Maxwell-Schrödinger equations [6, 17] with an initial seed of one atom in modes (1, 1) and (-1, -1), as shown by the dashed line in Fig. 4 with the coupling factor $g = 1.5 \times 10^6$. This simulation is in good qualitative agreement with our data but not completely satisfactory. The difference may be due to the necessity to take into account higher order modes in the scattering process and to go beyond 1D approximation. The matching condition of matter waves may also not be exactly satisfied. Describing this mechanism under full quantum methods [18] and considering wave mixing for the nonlinear high-order scattering modes is our future work.

To show the features of the position of the maximum and minimum of the scattering ratio vs the relative phase ϕ_0 , we simulate it for different pumping factors g in the weak coupling regime, as shown in Fig. 5. The backward scattering ratio increases with the coupling factor, which depends on the system parameters like the pump beam intensity and detuning, the total number of atoms or the BEC shape. The simulation clearly shows that the position of the maximum and minimum of the scattering very weakly depends on the experimental parameters, this is a generic feature. However, the value of the maximum increases with the coupling factor.

The superradiant scattering is initiated by quantum mechanical noise, i.e., spontaneous Rayleigh scattering from individual condensate atoms. Subsequent stimulated scattering and bosonic enhancement lead to rapid

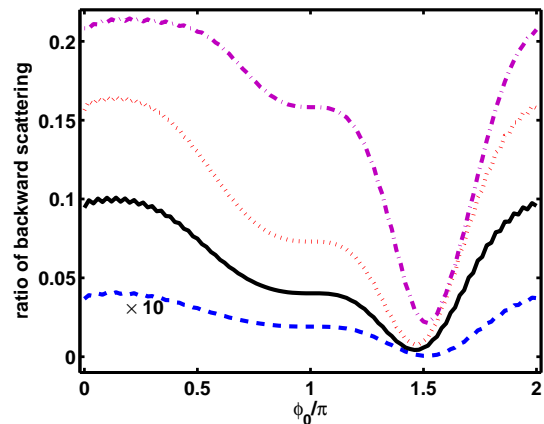


FIG. 5. The simulation for the ratio of backward scattered atoms to the total atom number vs the initial phase ϕ_0 for different weak coupling factors g : 1.0×10^6 (dashed line, its value is amplified by 10 times to show); 1.5×10^6 (solid line); 1.6×10^6 (dotted line) and 1.7×10^6 (dashed-dotted line).

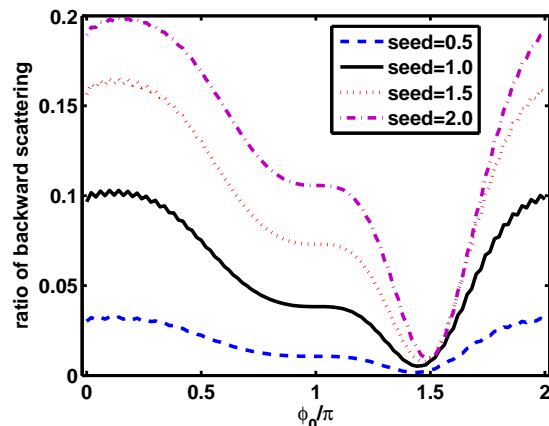


FIG. 6. The ratio of backward scattered atoms to the total atom number vs the initial phase ϕ_0 between the two pump beams for different seeds with $g = 1.5 \times 10^6$.

growth of the side-mode populations. The ratio of backward scattered atoms to the total atom number vs the initial phase for different initial seeds in modes (1, 1) and (-1, -1) are shown in Fig. 6. We can see that the positions of maximum and minimum do not vary with different seeds, although the amplitude of the scattering events changes obviously. The smaller the seeds, the lower the backward scattering amplitude. This shows that these features caused by the initial relative phase are not related to quantum fluctuation effects.

The above discussion is for the condition $\Delta\omega t = 2\pi$, which means identical coupling factor between light and atoms for the different initial relative phase. If the condition $\Delta\omega t = 2\pi$ is violated, the integration of the pump

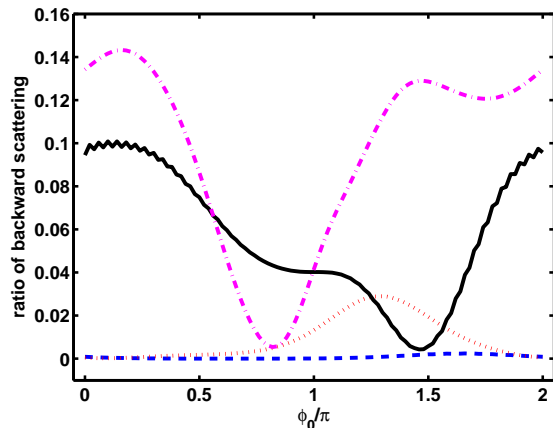


FIG. 7. The ratio of backward scattered atoms to the total atom number vs the initial phase ϕ_0 for the same frequency difference 15KHz but different pump times t : 22.22 μs (dashed line); 44.44 μs (dotted line); 66.67 μs (solid line) and 88.89 μs (dashed-dotted line). $g = 1.5 \times 10^6$.

intensity is different for different relative phases, so that the coupling factor is different. The ratio of backward scattered atoms to the total atom number vs the initial phase ϕ_0 is shown in Fig.7 for the same frequency dif-

ference 15KHz and different pump times t . From Fig. 7, we know that the position of the extrema will change at different t , while the value of the maximum will increase with t .

In summary, we have studied superradiant scattering from a Bose-Einstein condensate with a two-frequency pump beam. We have shown that this phenomenon depends much on the initial relative phase between the two optical components. Two matter gratings, one formed by the condensate at rest plus the side mode with positive momentum, the other by the condensate at rest plus the side mode with negative momentum, scatter endfire modes photons, which in the end affects the atom scattering process. We found that the relative optical phase is imprinted on matter wave gratings and can enhance or annihilate scattering in backward modes. Adjusting this phase provides a powerful tool for controlling superradiant scattering. It is already very beneficial for understanding the interaction between matter waves and optical waves in cooperative scattering.

We thank the anonymous referee for useful and detailed suggestions. This work is partially supported by the state Key Development Program for Basic Research of China (No.2005CB724503, 2006CB921401, 2006CB921402), NSFC (No.10874008, 10934010 and 60490280) and the Project-sponsored by SRF for ROCS, SEM.

-
- [1] S. Inouye, A. P. Chikkatur, D. M. Stamper-Kurn, J. Stenger, D. E. Pritchard, and W. Ketterle, *Science* **285**, 571 (1999).
 - [2] M. Kozuma, Y. Suzuki, Y. Torii, T. Sugiura, T. Kuga, E. W. Hagley, L. Deng, *Science* **286**, 2309 (1999).
 - [3] D. Schneble, Y. Torii, M. Boyd, E. W. Streed, D. E. Pritchard, and W. Ketterle, *Science* **300**, 475 (2003).
 - [4] Y. Yoshikawa, K. Nakayama, Y. Torii, T. Kuga, *Phys. Rev. Lett.* **99**, 220407 (2007).
 - [5] M. G. Moore and P. Meystre, *Phys. Rev. Lett.* **83**, 5202 (1999).
 - [6] O. Zobay and G. M. Nikolopoulos, *Phys. Rev. A* **73**, 013620 (2006), O. Zobay and G. M. Nikolopoulos, *Phys. Rev. A* **72**, 041604(R) (2005).
 - [7] H. Pu, W. Zhang and P. Meystre, *Phys. Rev. Lett.* **91**, 150407 (2003).
 - [8] Xu Xu, Xiaoji Zhou, Xuzong Chen, *Phys. Rev. A* **79**, 033605 (2009).
 - [9] L. E. Sadler, J. M. Higbie, S. R. Leslie, M. Vengalattore, and D. M. Stamper-Kurn, *Phys. Rev. Lett.* **98** 110401 (2007).
 - [10] S. Slama, S. Bex, G. Krenz, C. Zimmermann, Ph. W. Courteille, *Phys. Rev. Lett.* **98** 053603 (2007).
 - [11] S. Slama, G. Krenz, S. Bex, C. Zimmermann, Ph. W. Courteille, *Phys. Rev. A* **75** 063620 (2007).
 - [12] X. J. Zhou, *Phys. Rev. A* **80**, 023818 (2009).
 - [13] C. H. Van der Wal, M. D. Eisaman, A. Andre, R. L. Walseorth, D. F. Philips, A. S. Zibrov, M. D. Lukin, *Science* **301**, 196 (2003).
 - [14] D. N. Matsukevich, A. Kuzmich, *Science* **306**, 663 (2004).
 - [15] K. M. R. van der Stam, R. Meppelink, J. M. Vogels, J. W. Thomsen, and P. van der Straten, *cond-mat.other/0707.1465*.
 - [16] N. Bar-Gill, E. E. Rowen and N. Davidson, *Phys. Rev. A* **76**, 043603 (2007).
 - [17] F. Yang, X. J. Zhou, J. T. Li, Y. K. Chen, L. Xia, X. Z. Chen, *Phys. Rev. A* **78**, 043611 (2008).
 - [18] R. Guo, X. J. Zhou, X. Z. Chen, *Phys. Rev. A* **78**, 052107 (2008).